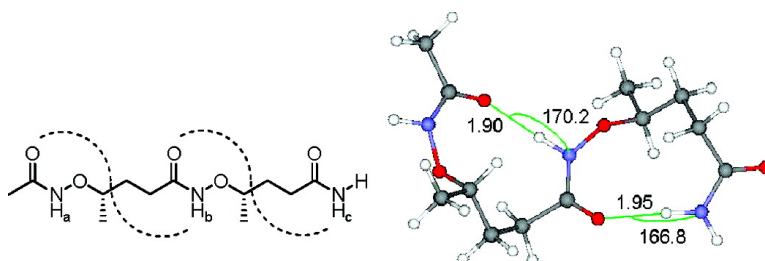


## Synthesis and Conformational Studies of $\alpha$ -Aminoxy Peptides

Fei Chen, Ke-Sheng Song, Yun-Dong Wu, and Dan Yang

*J. Am. Chem. Soc.*, **2008**, 130 (2), 743-755 • DOI: 10.1021/ja0772750

Downloaded from <http://pubs.acs.org> on February 8, 2009



### More About This Article

Additional resources and features associated with this article are available within the HTML version:

- Supporting Information
- Links to the 3 articles that cite this article, as of the time of this article download
- Access to high resolution figures
- Links to articles and content related to this article
- Copyright permission to reproduce figures and/or text from this article

[View the Full Text HTML](#)

## Synthesis and Conformational Studies of $\gamma$ -Aminoxy Peptides

Fei Chen,<sup>†</sup> Ke-Sheng Song,<sup>†</sup> Yun-Dong Wu,<sup>‡</sup> and Dan Yang<sup>\*†</sup>

Department of Chemistry, The University of Hong Kong, Pokfulam Road, Hong Kong, People's Republic of China, and Department of Chemistry, Hong Kong University of Science and Technology, Clear Water Bay, Kowloon, Hong Kong, People's Republic of China

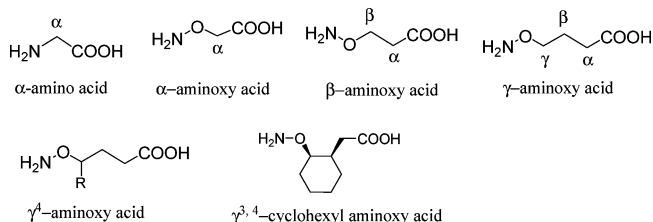
Received September 20, 2007; E-mail: yangdan@hku.hk

**Abstract:** We have synthesized a series of  $\gamma$ -aminoxy acids, including unsubstituted and  $\gamma^4$ -Ph-,  $\gamma^4$ -alkyl-, and  $\gamma^{3,4}$ -cyclohexyl-substituted systems. Coupling of these monomers to oligomers can be realized using EDCI/HOBt (or HOAt) as the coupling agent.  $\gamma$ -Aminoxy peptides can form 10-membered-ring intramolecular hydrogen bonds—so-called “ $\gamma$  N–O turns”—between adjacent residues, the extent of which is controlled by the nature of the side chain of each  $\gamma$ -aminoxy acid residue, increasing from the unsubstituted  $\gamma$ -aminoxy peptide to the  $\gamma^4$ -alkyl aminoxy peptides to the  $\gamma^4$ -phenyl- and  $\gamma^{3,4}$ -cyclohexyl-substituted aminoxy peptides. The presence of two consecutive homochiral 10-membered-ring intramolecular hydrogen bonds leads to the formation of a novel helical structure. Theoretical studies on a series of model peptides rationalize very well the experimentally observed conformational features of these  $\gamma$ -aminoxy peptides.

### Introduction

Peptidomimetic foldamers,<sup>1,2</sup> such as  $\beta$ -peptides,<sup>3–5</sup>  $\gamma$ -peptides,<sup>5,6</sup>  $\delta$ -peptides,<sup>7,8</sup> and aminoxy peptides,<sup>9–11</sup> attract much attention because of their unusual conformations and interesting bioactivities.<sup>12–15</sup> In a search for new peptidomimetic foldamers, we found that aminoxy peptides can feature strong intramolecular hydrogen bonds between adjacent residues (Chart 1). For example, peptides consisting of  $\alpha$ -aminoxy acids can possess eight-membered-ring intramolecular hydrogen bonds ( $\alpha$  N–O turns)<sup>9,16</sup> and peptides consisting of  $\beta$ -aminoxy acids can possess nine-membered-ring intramolecular hydrogen bonds ( $\beta$  N–O turns).<sup>10,17</sup> Oligomers of homochiral  $\alpha$ - or  $\beta$ -aminoxy acids can

Chart 1



form helical structures consisting of consecutive N–O turns (1.8<sub>8</sub> and 1.7<sub>9</sub> helices, respectively). Peptides containing  $\alpha$ -aminoxy acids are also good receptors for anions because of the acidity of their aminoxy amide protons.<sup>18,19</sup> A compound derived from an  $\alpha$ -aminoxy acid has been used as an effective chemical shift reagent for measuring the values of ee of carboxylic acids;<sup>20</sup> another compound derived from an  $\alpha$ -aminoxy acid can form chloride channels to mediate chloride ion transportation across cell membranes.<sup>21</sup> To enrich the category of aminoxy peptides and to test the ability of other aminoxy peptides to form local intramolecular hydrogen bonds, we sought to synthesize  $\gamma$ -aminoxy acid-based peptides and explore their conformational properties (Chart 1). Previously, we reported that  $\gamma^4$ -Ph aminoxy peptides can form turn and helix structures incorporating 10-membered-ring intramolecular hydrogen bonds ( $\gamma$  N–O turns).<sup>22</sup> Here we report the syntheses of a series of  $\gamma$ -aminoxy acid peptides—including unsubstituted and  $\gamma^4$ -Ph-,  $\gamma^4$ -alkyl-, and  $\gamma^{3,4}$ -

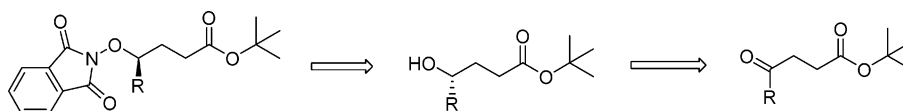
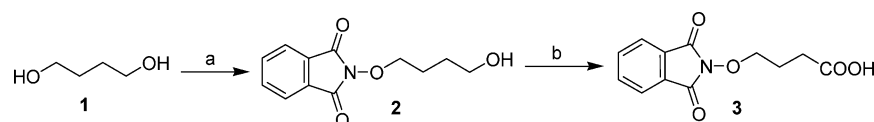
<sup>†</sup> The University of Hong Kong.

<sup>‡</sup> Hong Kong University of Science and Technology.

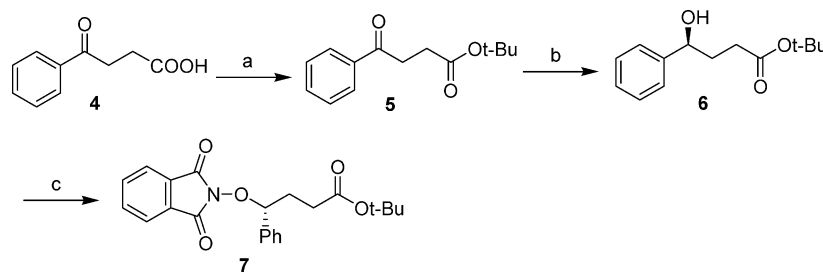
- Gellman, S. H. *Acc. Chem. Res.* **1998**, *31*, 173–180.
- Hill, D. J.; Mio, M. J.; Prince, R. B.; Hughes, T. S.; Moore, J. S. *Chem. Rev.* **2001**, *101*, 3893–4011.
- Cheng, R. P.; Gellman, S. H.; DeGrado, W. F. *Chem. Rev.* **2001**, *101*, 3219–3232.
- Seebach, D.; Matthews, J. L. *Chem. Commun.* **1997**, 2015–2022.
- Seebach, D.; Beck, A. K.; Bierbaum, D. J. *Chem. Biodivers.* **2004**, *1*, 1111–1239.
- Woll, M. G.; Lai, J. R.; Guzei, I. A.; Taylor, S. J. C.; Smith, M. E. B.; Gellman, S. H. *J. Am. Chem. Soc.* **2001**, *123*, 11077–11078.
- Gardner, R. R.; Liang, G. B.; Gellman, S. H. *J. Am. Chem. Soc.* **1999**, *121*, 1806–1816.
- Wipf, P.; Xiao, J. B. *Org. Lett.* **2005**, *7*, 103–106.
- Yang, D.; Ng, F. F.; Li, Z. J.; Wu, Y. D.; Chan, K. W. K.; Wang, D. P. *J. Am. Chem. Soc.* **1996**, *118*, 9794–9795.
- Yang, D.; Zhang, Y. H.; Zhu, N. Y. *J. Am. Chem. Soc.* **2002**, *124*, 9966–9967.
- Li, X.; Yang, D. *Chem. Commun.* **2006**, 3367–3379.
- Patch, J. A.; Barron, A. E. *Curr. Opin. Chem. Biol.* **2002**, *6*, 872–877.
- Sanford, A. R.; Gong, B. *Curr. Org. Chem.* **2003**, *7*, 1649–1659.
- Kritzer, J. A.; Stephens, O. M.; Guarracino, D. A.; Reznik, S. K.; Schepartz, A. *Bioorg. Med. Chem.* **2005**, *13*, 11–16.
- Goodman, C. M.; Choi, S.; Shandler, S.; Degrado, W. F. *Nat. Chem. Biol.* **2007**, *3*, 252–262.
- Yang, D.; Qu, J.; Li, B.; Ng, F. F.; Wang, X. C.; Cheung, K. K.; Wang, D. P.; Wu, Y. D. *J. Am. Chem. Soc.* **1999**, *121*, 589–590.
- Yang, D.; Zhang, Y. H.; Li, B.; Zhang, D. W.; Chan, J. C. Y.; Zhu, N. Y.; Luo, S. W.; Wu, Y. D. *J. Am. Chem. Soc.* **2004**, *126*, 6956–6966.

- Yang, D.; Li, X.; Sha, Y.; Wu, Y. D. *Chem. Eur. J.* **2005**, *11*, 3005–3009.
- Yang, D.; Qu, J.; Li, W.; Zhang, Y. H.; Ren, Y.; Wang, D. P.; Wu, Y. D. *J. Am. Chem. Soc.* **2002**, *124*, 12410–12411.
- Yang, D.; Li, X.; Fan, Y. F.; Zhang, D. W. *J. Am. Chem. Soc.* **2005**, *127*, 7996–7997.
- Li, X.; Shen, B.; Yao, X. Q.; Yang, D. *J. Am. Chem. Soc.* **2007**, *129*, 7264–7265.
- Chen, F.; Zhu, N. Y.; Yang, D. *J. Am. Chem. Soc.* **2004**, *126*, 15980–15981.

## Scheme 1

Scheme 2<sup>a</sup>

<sup>a</sup> Conditions: (a) DIAD, PPh<sub>3</sub>, PhthN-OH, THF, 1 h, 66% yield; (b) NaIO<sub>4</sub>, RuO<sub>2</sub>, CH<sub>3</sub>CN/H<sub>2</sub>O/EtOAc (15:10:3), 4 h, 80% yield.

Scheme 3<sup>a</sup>

<sup>a</sup> Conditions: (a) *t*-BuOH, DCC, DMAP, 12 h, CH<sub>2</sub>Cl<sub>2</sub>, 89% yield; (b) (–)-DIP-Cl, THF, –25 °C, 12 h, 95% yield, 97% ee; (c) PhthN-OH, PPh<sub>3</sub>, DEAD, THF, 1 h, 80% yield.

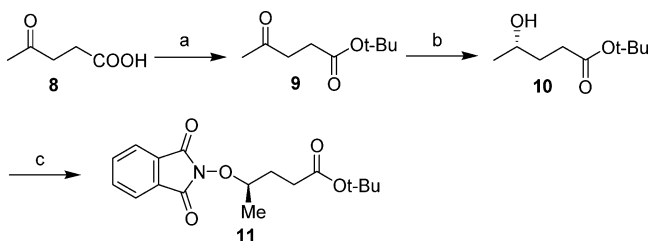
cyclohexyl-substituted systems—and our detailed conformational studies of those peptides using both experimental and theoretical approaches.

## Results and Discussion

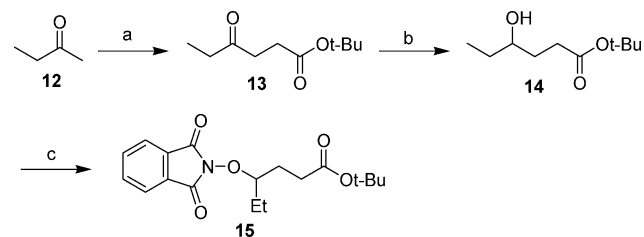
**Synthesis of  $\gamma$ -Aminoxy Peptides.** Scheme 1 presents a retrosynthetic analysis of a  $\gamma^4$ -aminoxy acid monomer. Generally, the ONH<sub>2</sub> and COOH groups of the aminoxy amide monomer are protected as phthalimidoxy and *tert*-butyl ester groups, respectively, which are readily removed using hydrazine hydrate and trifluoroacetic acid, respectively.<sup>23</sup> The phthalimidoxy group of the monomer can be readily introduced through a Mitsunobu reaction<sup>24</sup> between the  $\gamma$ -hydroxy ester and *N*-hydroxyphthalimide (PhthN-OH), with inversion of the configuration at the  $\gamma$  carbon atom. Previously, in syntheses of  $\beta$ -aminoxy acids, we encountered the problem of  $\alpha,\beta$ -elimination when attempting to introduce phthalimidoxy groups onto  $\beta$ -hydroxy esters; avoiding this problem required a long synthetic route.<sup>25</sup> For syntheses of  $\gamma$ -aminoxy acids, no such problem should be encountered, and a relatively short synthetic route can be envisioned. Furthermore, optical active  $\gamma$ -hydroxy esters can be prepared through asymmetric reduction of  $\gamma$ -keto esters.

We synthesized the unsubstituted  $\gamma$ -aminoxy acid monomer **3** from 1,4-butanediol **1** (Scheme 2). The Mitsunobu reaction of **1** with PhthN-OH afforded **2** in 66% yield. The oxidation of **2** with NaIO<sub>4</sub>, catalyzed by RuO<sub>2</sub>, gave the  $\gamma$ -aminoxy acid monomer **3** in 80% yield.

$\gamma^4$ -Aminoxy acids present a side chain at the C-4 position. We synthesized the  $\gamma^4$ -Ph aminoxy acid monomer **7** from 3-benzoylpropionic acid (**4**) according to the method outlined in Scheme 3. The carboxylic acid group of **4** was first protected

Scheme 4<sup>a</sup>

<sup>a</sup> Conditions: (a) *t*-BuOH, DCC, DMAP, CH<sub>2</sub>Cl<sub>2</sub>, 12 h, 46% yield; (b) Baker's yeast, sucrose, water, 3 d, 20% yield; (c) PhthN-OH, PPh<sub>3</sub>, DEAD, THF, 1 h, 78% yield, 99% ee.

Scheme 5<sup>a</sup>

<sup>a</sup> Conditions: (a) (i) LDA, THF, –78 to –20 °C, 1 h; (ii) *tert*-butyl  $\alpha$ -bromoacetate, –78 °C to room temp, 12 h, 42% yield; (b) NaBH<sub>4</sub>, THF/H<sub>2</sub>O, 1 h; (c) PhthN-OH, PPh<sub>3</sub>, DEAD, THF, 1 h, 56% yield, two steps.

as  $\gamma$ -keto *tert*-butyl ester **5**, reduction of which using (–)-DIP-Cl<sup>26</sup> gave the optically active  $\gamma$ -hydroxy ester **6** in 95% yield and 97% ee. The Mitsunobu reaction of **6** with PhthN-OH resulted in inversion of configuration at the  $\gamma$  carbon atom, affording chiral  $\gamma$ -aminoxy acid monomer **7** in 80% yield.

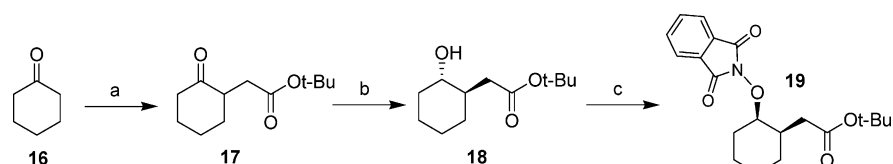
For the synthesis of alkyl substituted chiral  $\gamma$ -hydroxy esters, the DIP-Cl reduction method was not applicable because it requires the presence of a phenyl group on the  $\gamma$ -keto group to achieve a high ee.<sup>26</sup> Instead, we chose baker's yeast as a

(23) Yang, D.; Li, B.; Ng, F. F.; Yan, Y. L.; Qu, J.; Wu, Y. D. *J. Org. Chem.* **2001**, *66*, 7303–7312.

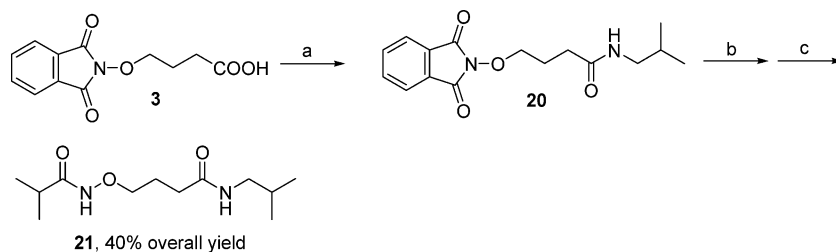
(24) Mitsunobu, O. *Synthesis* **1981**, 1–28.

(25) Yang, D.; Zhang, Y. H.; Li, B.; Zhang, D. W. *J. Org. Chem.* **2004**, *69*, 7577–7581.

(26) Ramachandran, P. V.; Pitre, S.; Brown, H. C. *J. Org. Chem.* **2002**, *67*, 5315–5319.

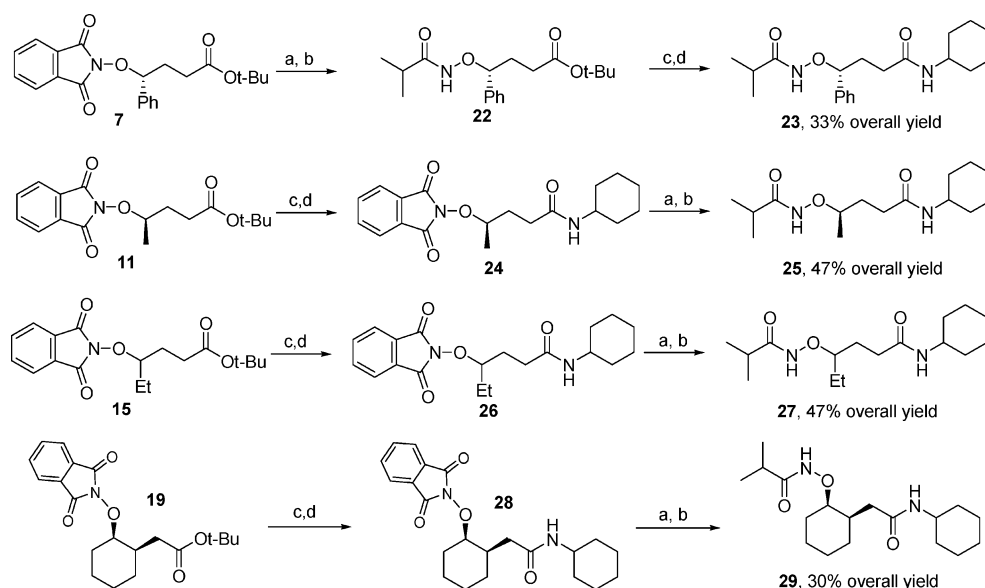
Scheme 6<sup>a</sup>

<sup>a</sup> Conditions: (a) (i) LDA, THF,  $-78$  to  $-20$  °C, 1 h; (ii) *tert*-butyl  $\alpha$ -bromoacetate,  $-78$  °C to room temp, 12 h, 80% yield; (b) Baker's yeast, sucrose, water, 3 d, 26% yield; (c) PhthN-OH, PPh<sub>3</sub>, DEAD, THF, 1 h, 40% yield, 98% ee.

Scheme 7<sup>a</sup>

21, 40% overall yield

<sup>a</sup> Conditions: (a) EDCI, HOAt, isobutylamine, CH<sub>2</sub>Cl<sub>2</sub>; (b) NH<sub>2</sub>NH<sub>2</sub>, MeOH/CH<sub>2</sub>Cl<sub>2</sub>; (c) EDCI, HOAt, isobutyric acid, CH<sub>2</sub>Cl<sub>2</sub>.

Scheme 8<sup>a</sup>

<sup>a</sup> Conditions: (a) NH<sub>2</sub>NH<sub>2</sub>, MeOH/CH<sub>2</sub>Cl<sub>2</sub>; (b) EDCI, HOBT, isobutyric acid, CH<sub>2</sub>Cl<sub>2</sub>; (c) TFA, CH<sub>2</sub>Cl<sub>2</sub>; (d) EDCI, HOBT, cyclohexylamine, CH<sub>2</sub>Cl<sub>2</sub>.

biocatalyst because it is a common microorganism for the asymmetric reduction of carbonyl compounds.<sup>27</sup>

We synthesized the  $\gamma^4$ -Me aminoxy acid monomer **11** from 4-oxopentanoic acid **8** (Scheme 4). The carboxylic group of **8** was protected in the form of the  $\gamma$ -keto *tert*-butyl ester **9**, which we reduced using baker's yeast to afford the chiral  $\gamma$ -hydroxy ester **10** in 20% yield. The relatively low yield of this step was probably due to the incompatibility of *t*-Bu group with baker's yeast or the poor solubility of substrate **9**. The Mitsunobu reaction of **10** with PhthN-OH yielded the  $\gamma^4$ -Me aminoxy acid monomer **11** in 78% yield and 99% ee.

We synthesized the  $\gamma^4$ -Et aminoxy acid monomer following the route illustrated in Scheme 5. Butanone was first deprotonated using LDA and then reacted with *tert*-butyl  $\alpha$ -bromoacetate to afford the  $\gamma$ -keto ester **13**, reduction of which using NaBH<sub>4</sub> gave the  $\gamma$ -hydroxy ester **14**. The Mitsunobu reaction

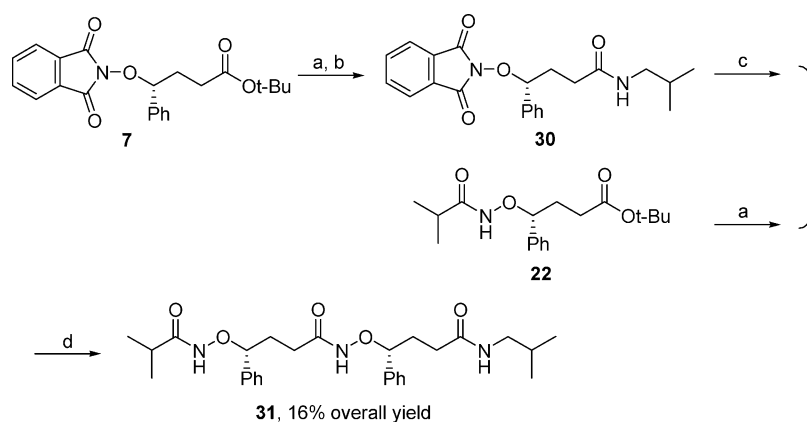
of **14** with PhthN-OH afforded **15** in 60% yield. Reduction of **13** with baker's yeast gave the chiral  $\gamma$ -hydroxy ester **14** and the chiral monomer **15**, but the ee of **15** was a disappointing 55%. Therefore, we used NaBH<sub>4</sub> to reduce **13** to **14**, and employed the racemic sample of the  $\gamma^4$ -Et aminoxy amide for our conformational studies.

We synthesized the chiral  $\gamma^{3,4}$ -cyclohexyl aminoxy acid monomer **19** from cyclohexanone (Scheme 6). Cyclohexanone (**16**) was first deprotonated using LDA and then reacted with *tert*-butyl  $\alpha$ -bromoacetate to afford the  $\gamma$ -keto ester **17** in 80% yield. Asymmetric reduction of **17** using baker's yeast gave the optically active  $\gamma$ -hydroxy ester **18** in 26% yield.<sup>28</sup> After a Mitsunobu reaction, the final chiral product **19** was obtained in 40% yield and 98% ee.

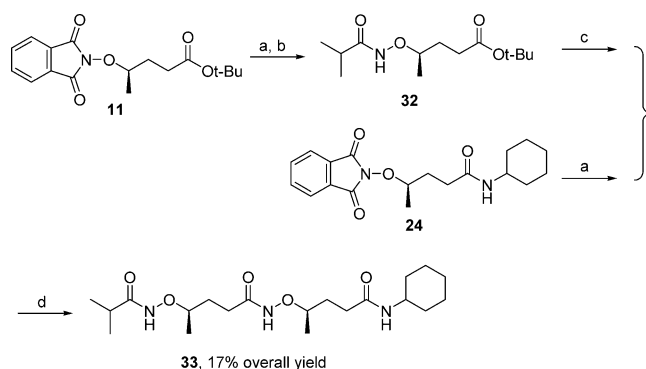
Following our previously reported protocol<sup>23</sup> for  $\alpha$ -aminoxy peptide synthesis using EDCI/HOBt (or HOAt) as the coupling

(27) Ema, T.; Sugiyama, Y.; Fukumoto, M.; Moriya, H.; Cui, J. N.; Sakai, T.; Utsuka, M. *J. Org. Chem.* **1998**, *63*, 4996–5000.

(28) Ganaha, M.; Funabiki, Y.; Motoki, M.; Yamauchi, S.; Kinoshita, Y. *Biosci. Biotechnol. Biochem.* **1998**, *62*, 181–184.

Scheme 9<sup>a</sup>

<sup>a</sup> Conditions: (a) TFA, CH<sub>2</sub>Cl<sub>2</sub>; (b) EDCI, HOBT, isobutylamine, CH<sub>2</sub>Cl<sub>2</sub>; (c) NH<sub>2</sub>NH<sub>2</sub>, MeOH, CH<sub>2</sub>Cl<sub>2</sub>; (d) EDCI, HOBT, CH<sub>2</sub>Cl<sub>2</sub>.

Scheme 10<sup>a</sup>

<sup>a</sup> Conditions: (a) NH<sub>2</sub>NH<sub>2</sub>, MeOH, CH<sub>2</sub>Cl<sub>2</sub>; (b) EDCI, HOBT, isobutyric acid, CH<sub>2</sub>Cl<sub>2</sub>; (c) TFA, CH<sub>2</sub>Cl<sub>2</sub>; (d) EDCI, HOBT, CH<sub>2</sub>Cl<sub>2</sub>.

agent, we coupled the monomers **3**, **7**, **11**, **15**, and **19** to form the diamides **21** (Scheme 7), **23**, **25**, **27**, and **29** (Scheme 8) and the triamides **31** (Scheme 9) and **33** (Scheme 10). Below, we discuss our detailed conformational studies of these compounds; we have previously communicated some conformational studies of **21**, **23**, and **31** (Chart 2).<sup>22</sup>

Two <sup>1</sup>H NMR spectroscopic methods, dilution<sup>29</sup> and DMSO-*d*<sub>6</sub> addition,<sup>30,30</sup> are applied to probe the formation of intramolecular hydrogen bonds in the oligomers of  $\gamma$ -aminoxy acids (Chart 2). The <sup>1</sup>H NMR dilution study is to monitor the chemical shift changes of amide protons with respect to peptide concentration, and the <sup>1</sup>H NMR DMSO-*d*<sub>6</sub> addition study is to follow the chemical shift changes of amide protons with respect to the content of DMSO-*d*<sub>6</sub> added. Data for the <sup>1</sup>H NMR dilution study of amide proton NH<sub>c</sub> of **31** and the <sup>1</sup>H NMR DMSO-*d*<sub>6</sub> addition studies of amide protons NH<sub>b</sub> of **23** and NH<sub>c</sub> of **31** are not presented here because the chemical shift values of these protons overlapped with the chemical shift values of phenyl protons in these molecules.

Table 1 summarizes the chemical shifts of the amide protons of **21**, **23**, **25**, **27**, **29**, **31**, and **33** and their chemical shift changes (Figure 1) in <sup>1</sup>H NMR spectroscopic dilution and DMSO-*d*<sub>6</sub> addition studies at room temperature. The chemical shifts of the *N*-oxy amide protons NH<sub>a</sub> of these compounds at 0.78 mM were located considerably upfield (7.81–8.62 ppm), with

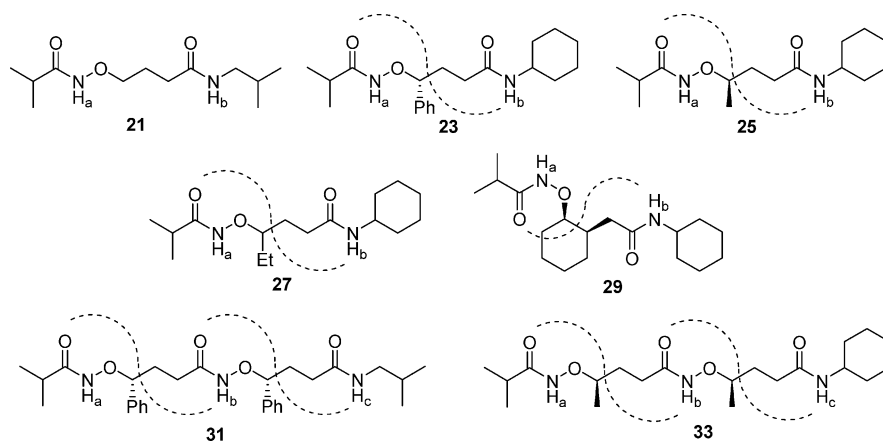
relatively large chemical shift changes in both the <sup>1</sup>H NMR spectroscopic dilution ( $\Delta\delta = 0.70$ – $1.37$  ppm) and DMSO-*d*<sub>6</sub> addition ( $\Delta\delta = 1.66$ – $2.30$  ppm) studies, suggesting that no strong intramolecular hydrogen bonds were formed using these protons. Similarly, the chemical shift of the NH<sub>b</sub> proton of **21** at 0.78 mM was located quite far upfield (6.20 ppm), with relatively large chemical shift changes in both the <sup>1</sup>H NMR spectroscopic dilution ( $\Delta\delta = 0.56$  ppm) and DMSO-*d*<sub>6</sub> addition ( $\Delta\delta = 0.91$  ppm) studies, again suggesting that this proton was not involved in any strong intramolecular hydrogen bonds.

The chemical shifts of the NH<sub>b</sub> protons of **23**, **25**, **27**, **29**, **31**, and **33** and the NH<sub>c</sub> proton of **33** were located rather downfield (7.05, 6.45, 6.39, 7.02, 10.57, 10.43, and 6.90 ppm, respectively) and underwent relatively small changes in the <sup>1</sup>H NMR spectroscopic dilution ( $\Delta\delta < 0.4$  ppm) and DMSO-*d*<sub>6</sub> addition ( $\Delta\delta < 0.9$  ppm) studies, revealing that these amide protons were parts of 10-membered-ring intramolecular hydrogen bonds between C=O<sub>*i*</sub> and NH<sub>*i*+2</sub> groups, that is,  $\gamma$  N–O turns. We noted that the chemical shifts of the NH<sub>b</sub> protons in **25** (6.45 ppm) and **27** (6.39 ppm) were located less downfield than those in **23** (7.05 ppm) and **29** (7.02 ppm), suggesting that the NH<sub>b</sub> protons in **25** and **27** formed weaker intramolecular hydrogen bonds than did those in **23** and **29**. This situation arose because one of the driving forces for the formation of a 10-membered-ring intramolecular hydrogen bond is the gauche orientation of the C <sub>$\gamma$</sub> –O bond relative to the C <sub>$\alpha$</sub> –C <sub>$\beta$</sub>  bond. For **23**, the phenyl group at the  $\gamma$  position favors an anti orientation relative to the C <sub>$\alpha$</sub> –C <sub>$\beta$</sub>  bond, which results in a gauche orientation of the C <sub>$\gamma$</sub> –O bond relative to the C <sub>$\alpha$</sub> –C <sub>$\beta$</sub>  bond. For **29**, the cyclohexane ring has already restricted the C <sub>$\gamma$</sub> –O bond to be positioned gauche to the C <sub>$\alpha$</sub> –C <sub>$\beta$</sub>  bond. For **25** and **27**, however, the alkyl substituent at the  $\gamma$  position is relatively small; it cannot control very well the gauche orientation of the C <sub>$\gamma$</sub> –O bond relative to the C <sub>$\alpha$</sub> –C <sub>$\beta$</sub>  bond and, thus, weaker 10-membered-ring intramolecular hydrogen bonds exist in **25** and **27** relative to those in **23** and **29**.

The chemical shift of the NH<sub>c</sub> proton in **33** was located further downfield (6.90 ppm) than that of the NH<sub>b</sub> proton in **25** (6.45 ppm), which indicates that the intramolecular hydrogen bond in **33** is stronger than that in **25**, suggesting that the intramolecular hydrogen bond of the NH<sub>c</sub> proton was strengthened after elongation of the peptide chain from the diamide **25** to the triamide **33**; that is, the formation of consecutive 10-membered-ring intramolecular hydrogen bonds is a cooperative process.

(29) Haque, T. S.; Little, J. C.; Gellman, S. H. *J. Am. Chem. Soc.* **1994**, *116*, 4105–4106.

(30) Copeland, G. T.; Jarvo, E. R.; Miller, S. J. *J. Org. Chem.* **1998**, *63*, 6784–6785.

**Chart 2.**  $^1\text{H}$  NMR Spectroscopic Studies of  $\gamma$ -Aminoxy Peptides**Table 1.** Chemical Shifts ( $\delta_{\text{NH}}$ ) and Chemical Shift Changes ( $\Delta\delta_{\text{NH}}$ ) of Amide Protons in  $^1\text{H}$  NMR Spectroscopic Dilution (dilu.) and DMSO- $d_6$  Addition (DMSO) Studies of Peptides **21**, **23**, **25**, **27**, **29**, **31**, and **33** at 25 °C

	$\text{NH}_a$ (ppm)			$\text{NH}_b$ (ppm)			$\text{NH}_c$ (ppm)		
	$\delta^a$	$\Delta\delta^b$	$\Delta\delta^c$	$\delta^a$	$\Delta\delta^b$	$\Delta\delta^c$	$\delta^a$	$\Delta\delta^b$	$\Delta\delta^c$
		(dilu.)	(DMSO)		(dilu.)	(DMSO)		(dilu.)	(DMSO)
<b>21</b>	8.62	1.06	1.66	6.20	0.56	0.91			
<b>23</b>	7.94	0.82	2.15	7.05	0.2	<i>d</i>			
<b>25</b>	8.45	0.81	1.87	6.45	0.39	0.82			
<b>27</b>	8.48	0.70	1.75	6.39	0.38	0.86			
<b>29</b>	8.37	0.83	1.96	7.02	0.39	0.73			
<b>31</b>	7.81	1.07	2.30	10.57	0.2	0.34			
<b>33</b>	8.33	1.37	2.10	10.43	0.33	0.35	6.90	0.25	0.32

<sup>a</sup>  $\delta$ : Amide NH proton's chemical shift obtained from the  $^1\text{H}$  NMR spectrum of the indicated compound at a concentration of 0.78 mM in  $\text{CDCl}_3$ . <sup>b</sup> The value of  $\Delta\delta$  in the dilution studies was calculated using the equation  $\Delta\delta = \delta_{\text{NH}}(100 \text{ mM}) - \delta_{\text{NH}}(0.78 \text{ mM})$ . <sup>c</sup> The value of  $\Delta\delta$  in the DMSO- $d_6$  addition studies was calculated using the equation  $\Delta\delta = \delta_{\text{NH}}(9\% \text{ DMSO-}d_6 \text{ in } \text{CDCl}_3) - \delta_{\text{NH}}(\text{CDCl}_3)$ . <sup>d</sup> The signal overlapped with the aromatic protons after the addition of DMSO.

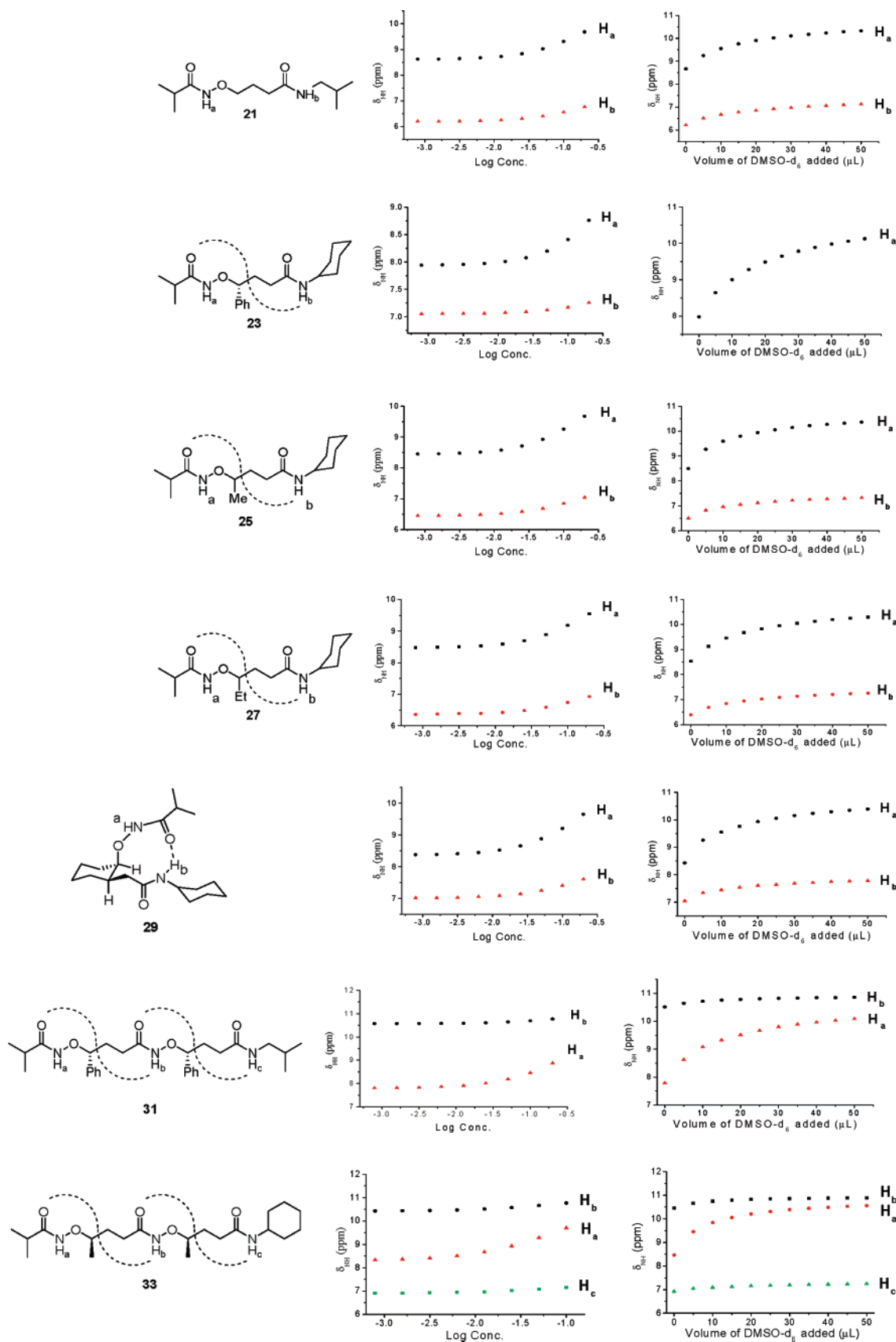
**IR Spectroscopic Studies of  $\gamma$ -Aminoxy Peptides.** Data from the N–H stretching region in IR spectra can provide insight into the degree of hydrogen bond formation in nonpolar solvents because the time scale of IR spectroscopic measurements is sufficiently short to distinguish clearly between the N–H stretchings of hydrogen-bonded and non-hydrogen-bonded states. According to our previous studies, the IR spectral absorption bands of the non-hydrogen-bonded amide N–H and N-oxy amide N–H bonds appear in the regions 3450–3400 and 3400–3340  $\text{cm}^{-1}$ , respectively, while the absorption bands corresponding to the hydrogen-bonded amide N–H and N-oxy amide N–H bonds appear at wavenumbers less than 3370 and 3250  $\text{cm}^{-1}$ , respectively.<sup>17</sup>

Figure 2 presents the N–H stretching regions of the FT-IR spectra of **21**, **23**, **25**, **27**, **29**, **31**, and **33**. The spectra were recorded for these samples in dichloromethane at a concentration (2 mM) at which intermolecular hydrogen bonding is unlikely to occur. For **21**, we observed two major bands (3446 and 3392  $\text{cm}^{-1}$ , assigned to the stretching frequencies of the non-hydrogen-bonded amide  $\text{NH}_b$  and  $\text{NH}_a$  bonds) and two minor bands (3338 and 3280  $\text{cm}^{-1}$ , assigned to the stretchings of the hydrogen-bonded  $\text{NH}_b$  and  $\text{NH}_a$  bonds). The presence of a minor intramolecular hydrogen-bonded amide band for the  $\text{NH}_b$  bond of **21** indicates that the 10-membered-ring intramolecular hydrogen-bonded conformation did not predominate.

For compounds **23**, **25**, **27**, and **29**, we observed three main sets of peaks, which we assigned to the stretching frequencies of the non-hydrogen-bonded amide  $\text{NH}_b$  (3428, 3430, 3429, and 3420  $\text{cm}^{-1}$ ), non-hydrogen-bonded N-oxy amide  $\text{NH}_a$  (3388, 3392, 3391, and 3386  $\text{cm}^{-1}$ ), and hydrogen-bonded amide  $\text{NH}_b$  (3324, 3320, 3322, and 3316  $\text{cm}^{-1}$ ) bonds, respectively. The presence of major hydrogen-bonded amide  $\text{NH}_b$  and minor non-hydrogen-bonded amide  $\text{NH}_b$  bands in **23** and **29** indicates that they adopt extensive 10-membered ring intramolecular hydrogen bond conformations. The relatively smaller hydrogen-bonded and the relatively larger non-hydrogen-bonded amide  $\text{NH}_b$  bands in **25** and **27**, compared with those in **23** and **29**, suggest that the tendency of **25** and **27** to experience 10-membered-ring intramolecular hydrogen bond formation is weaker than that of **23** and **29**. In addition, the relatively larger hydrogen-bonded and relatively smaller non-hydrogen-bonded amide  $\text{NH}_b$  bands in **25** and **27**, compared with those for **21**, indicate that the tendency of **25** and **27** to experience 10-membered-ring intramolecular hydrogen bond formation is stronger than that of **21**.

It is interesting to note that there were small bands in the region 3200–3300  $\text{cm}^{-1}$  in the IR spectra of **21**, **25**, and **27**. We assign these bands to the stretching frequencies of the hydrogen-bonded  $\text{NH}_a$  groups, which suggests the formation of eight-membered-ring intramolecular hydrogen bonds between the N-oxy amide  $\text{NH}_i$  and  $\text{C}=\text{O}_i$  groups in **21**, **25**, and **27** (Figure 3).

For the triamides **31** and **33**, we observed four bands (3441, 3387, 3325, and 3211  $\text{cm}^{-1}$  for **31**; 3428, 3394, 3300, and 3214  $\text{cm}^{-1}$  for **33**), which we assign to the stretching frequencies of the non-hydrogen-bonded amide  $\text{NH}_c$  (3441 and 3428  $\text{cm}^{-1}$ ), the non-hydrogen-bonded N-oxy amide  $\text{NH}_a$  and  $\text{NH}_b$  (3387 and 3394  $\text{cm}^{-1}$ ), the hydrogen-bonded amide  $\text{NH}_c$  (3325 and 3300  $\text{cm}^{-1}$ ), and the hydrogen-bonded N-oxy amide  $\text{NH}_a$  and  $\text{NH}_b$  (3211 and 3214  $\text{cm}^{-1}$ ) bonds, respectively. The large hydrogen-bonded amide  $\text{NH}_c$  bands and the small non-hydrogen-bonded amide  $\text{NH}_c$  bands indicate that the  $\text{NH}_c$  groups of **23** and **29** exist mainly in 10-membered-ring intramolecular hydrogen bond conformations. Considering that the  $\text{NH}_a$  groups did not form intramolecular hydrogen bonds and that the  $\text{NH}_b$  groups formed intramolecular hydrogen bonds (according to the results of our  $^1\text{H}$  NMR spectroscopy studies), the bands at 3387 and 3394  $\text{cm}^{-1}$  can be assigned primarily to the signals of the



**Figure 1.** (Left-hand column) Amide proton chemical shifts plotted as a function of the logarithm of the concentration of peptides **21**, **23**, **25**, **27**, **29**, **31**, and **33** in  $\text{CDCl}_3$  at room temperature; (right-hand column) amide proton chemical shifts plotted as a function of the amount of  $\text{DMSO-}d_6$  added to 5 mM solutions of peptides **21**, **23**, **25**, **27**, **29**, **31**, and **33** in  $\text{CDCl}_3$  (0.5 mL) at room temperature.

non-hydrogen-bonded *N*-oxy amide  $\text{NH}_a$  groups and those at 3325 and 3300  $\text{cm}^{-1}$  can be assigned primarily to the signals

of hydrogen-bonded  $\text{NH}_b$  groups; thus, the existence of two consecutive 10-membered-ring intramolecular hydrogen bonds

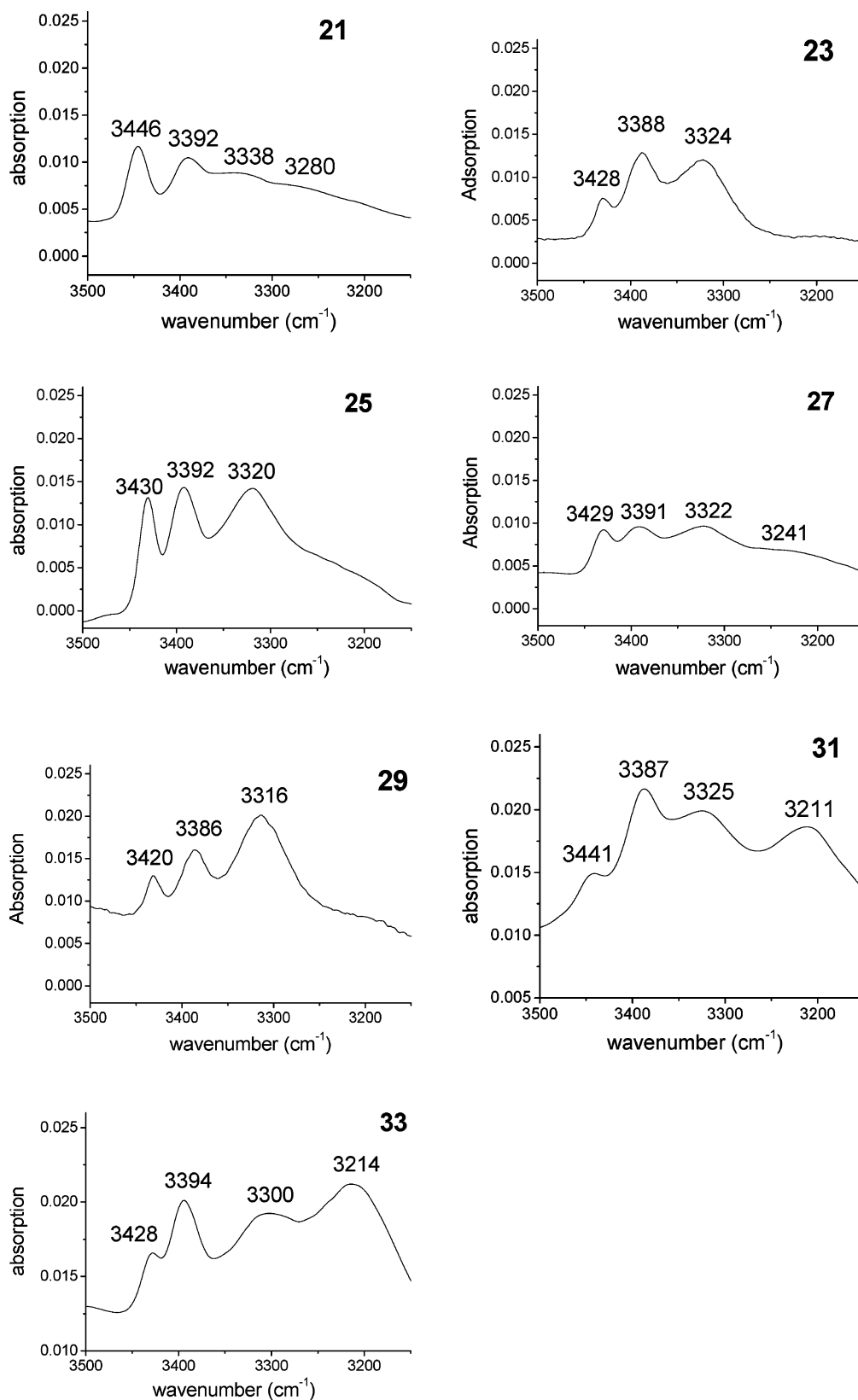


**Figure 2.** N–H Stretching regions of the FT-IR spectra of **21**, **23**, **25**, **27**, **29**, **31**, and **33** (2 mM in  $\text{CH}_2\text{Cl}_2$ ) at room temperature (after subtraction of the spectrum of pure  $\text{CH}_2\text{Cl}_2$ ).

predominates for the conformations of **31** and **33** in  $\text{CH}_2\text{Cl}_2$  solution.

**2D-NOESY Studies of  $\gamma$ -Aminoxy Peptides.** We performed 2D-NOESY studies of **21**, **23**, **25**, and **29** in  $\text{CDCl}_3$  to probe their conformations in solution (Figure 4). Because of their

overlapping signals, no 2D-NOESY spectra were recorded for **27**, **31**, and **33**. For **23**, **25**, and **29**, we detected obvious NOE signals between  $\text{H}_b$  and the  $\gamma$  proton, but no such signal for **21**. This finding suggests that the backbones of **23**, **25**, and **29** were bent, while that of **21** was not.



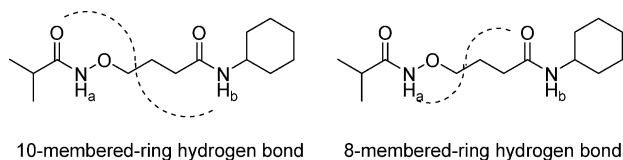


**Figure 3.** Two possible intramolecular hydrogen bonds within a  $\gamma$ -aminoxy peptide.

**CD Studies of  $\gamma$ -Aminoxy Peptides.** Circular dichroism (CD) spectroscopy has been used successfully to characterize the secondary structures of natural peptides<sup>31–33</sup> and unnatural peptides such as  $\beta$ -peptides<sup>4,34–36</sup> and aminoxy peptides.<sup>16,17,22,23,37</sup> Figure 5 presents the CD spectra of **23**, **25**, **29**, **31**, and **33** recorded at room temperature in 2,2,2-trifluoroethanol (TFE); these CD signals have been normalized with respect to the concentration and number of backbone N–O turns of each compound. In the CD spectrum of **29**, a strong absorption peak appeared at 203 nm; its intensity was similar to that of the broad peaks at ca. 210 nm in the spectra of **23** and **31**.<sup>22</sup> In contrast, for **25** and **33** we observed only weak broad peaks between 205 and 230 nm. The lower intensity of these two peaks is probably due to the conformational flexibility of **25** and **33**, in which the  $\gamma^4$ -Me group does not exert a strong influence on the secondary structures.

**Theoretical Calculations.** To further understand the conformational features of the unsubstituted  $\gamma$ -aminoxy and  $\gamma^4$ -Me-,  $\gamma^4$ -Et-,  $\gamma^4$ -Ph-, and  $\gamma^{3,4}$ -cyclohexyl-substituted aminoxy peptides, we performed theoretical calculations on the model compounds **34–39** (Figure 6) using the Gaussian 98 software package.<sup>38</sup> All of the geometries were fully optimized using the B3LYP<sup>39,40</sup>/6-31G (d, p) method followed by harmonic vibration frequency calculations to ensure that each structure was a minimum. Energies were evaluated through MP2<sup>41–43</sup>/6-31G (d, p) calculations on the B3LYP/6-31G (d, p) geometries. The effect of solvent was evaluated by the PCM model using the B3LYP/6-31G (d, p) method. A dielectric constant of 8.93 was set to model CH<sub>2</sub>Cl<sub>2</sub> as solvent. The relative free energies of the conformers were calculated with the MP2/6-31G (d, p) energies plus the enthalpy and entropy corrections along with the solvent energy corrections, as shown in eq 1.

$$\Delta G = \Delta E(\text{MP2}) + [\Delta E(\text{B3LYP, solvent}) - \Delta E(\text{B3LYP})] + \text{enthalpy correction} - T\Delta S \quad (1)$$

Figure 7 displays the five most stable conformations of model compound **34**. Ten-membered-ring hydrogen bonds are found in conformers **34a–c**, of which **34a** is the most stable (hydrogen bond length: 2.00 Å; hydrogen bond angle: 163.0°); conformers **34b** and **34c** are less stable because of their unfavorable torsional angles  $\varphi$  and  $\phi$ , respectively (see Table 2). Conformer **34d**, having an eight-membered-ring hydrogen bond, has a similar

stability to that of **34a**. Conformer **34e**, with its extended backbone, is less stable than those conformers that feature intramolecular hydrogen bonds. Overall, the calculations predict that compound **34** can adopt both eight- and 10-membered-ring hydrogen bond conformations, which would exist in equilibrium. This finding is corroborated by the experimental results. For example, in the IR spectrum of the unsubstituted  $\gamma$ -aminoxy peptide **21**, the peaks appearing at 3392 and 3338 cm<sup>-1</sup> correspond to the free aminoxy amide NH<sub>a</sub> and the 10-membered-ring hydrogen-bonded amide NH<sub>b</sub> units, respectively, whereas the signals at 3346 and 3280 cm<sup>-1</sup> correspond to the free amide NH<sub>b</sub> and the eight-membered-ring hydrogen-bonded amide NH<sub>a</sub> units, respectively.

With a methyl group introduced to the  $\gamma$  carbon atom in an (*S*)-configuration, model compound **35** can adopt several conformations; Figure 8 displays the six most stable of them. Conformer **35a**, which is derived from **34a**, but with a shorter hydrogen bond length and a better hydrogen bond angle, is the most stable. Conformers **35b** and **35c**, which are derived from **34b** and **34c**, respectively, are less stable than conformer **35a**. It is notable that while **34b** is less stable than **34c**, **35b** is more stable than **35c**, presumably because the methyl group is gauche to the N–O bond in **35b** (with a distance of 2.74 Å between one hydrogen atom on the methyl group and the aminoxy amide proton), whereas it is gauche to the C<sub>α</sub>–C<sub>β</sub> bond in **35c** (with a distance of 2.47 Å between one hydrogen atom on the methyl group and the C<sub>α</sub> hydrogen atom). Obviously, the degree of steric repulsion is stronger in **35c** than it is in **35b**. Conformers **35d** and **35e**, with their eight-membered-ring hydrogen bonds, and the extended conformer **35f** are also less stable than conformer **35a**. Conformer **35d** is more stable than **35e** because the methyl group is aligned anti to the N–O bond in **35d**, while the C<sub>γ</sub>–H bond is eclipsed with the N–O bond in **35e**. Interestingly, the energy difference between **35a** and **35d** is larger than that between **34a** and **34d**, presumably because the methyl group is gauche to the N–O bond in **35a** (with a distance of 2.73 Å between one hydrogen atom on the methyl group and the amide hydrogen atom), whereas it is gauche to the C<sub>α</sub>–C<sub>β</sub> bond in **35d** (with a distance of 2.29 Å between one hydrogen atom on the methyl group and the C<sub>α</sub> hydrogen atom), resulting in stronger steric repulsion in **35d** than in **35a**. As a result, the energy increase from **34d** to **35d** is higher than that from **34a** to **35a**. These results suggest that the  $\gamma^4$ -Me aminoxy model compound **35** having the (*S*)-configuration favors the left-handed 10-membered-ring hydrogen bond conformation, but because the free energy difference between the dominant conformer **35a** and conformer **35d** is not large (0.7 kcal/mol), their interconversion is facile. Our experimental results for compound **25** indicate that the 10-membered-ring hydrogen bond is favored

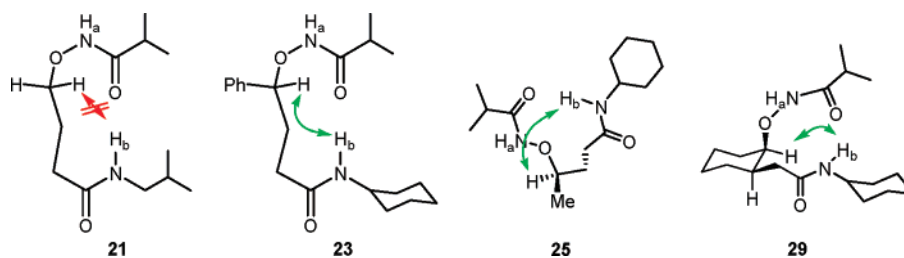


**Figure 4.**

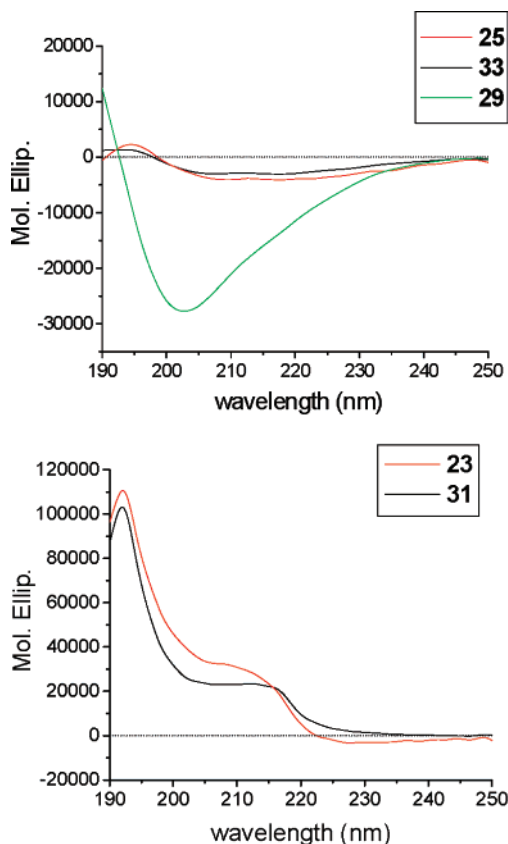


**Figure 5.** CD spectra of peptides **25** (0.1 mM in TFE) and **23**, **29**, **31**, and **33** (0.4 mM in TFE) at 25 °C.

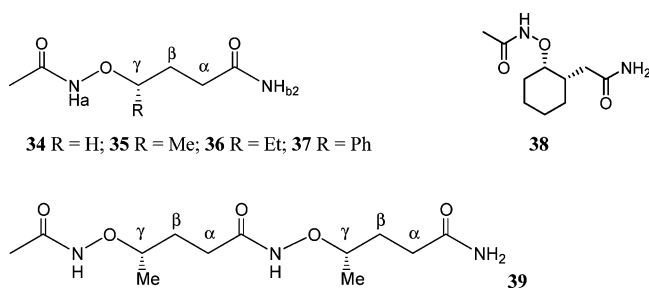


**Figure 6.** Model  $\gamma$ -aminoxy peptides **34**–**39**.

**Table 2.** Torsional Angles of  $\gamma$ -Aminoxy Peptides Optimized Using B3LYP/6-31G (d, p)

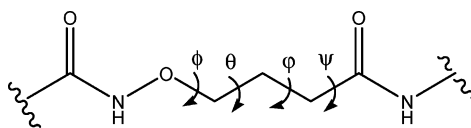
**34a** 0.0 (0.0)      **34b** 1.4 (1.4)      **34c** 1.1 (0.9)

**34d** 0.2 (0.0)      **34e** 2.8 (1.4)

**Figure 7.** Calculated conformers of model compound **34**. The calculated relative free energies (kcal/mol) in the gas phase and in CH<sub>2</sub>Cl<sub>2</sub> (in parentheses) and the N–H···O hydrogen bond lengths and angles are provided.

over the 8-membered-ring hydrogen bond (stronger signals at 3392 and 3320 cm<sup>-1</sup> than that at 3430 cm<sup>-1</sup>).

The conformations of compound **36** can be derived from those of compound **35** by replacing one of the hydrogen atoms on the C<sub>γ</sub> methyl group with a methyl group. Figure 9 indicates that the relative stabilities of the most stable conformers of compound **36** are similar to those of compound **35**. One notable change is that the calculated free energy difference between **36a** and **36d** is ca. 0.1 kcal/mol in CH<sub>2</sub>Cl<sub>2</sub>, while the corresponding energy difference between **35a** and **35d** is ca. 0.7 kcal/mol. In both **36a** and **36d**, the additional methyl group is aligned gauche to the C<sub>β</sub>–C<sub>γ</sub> bond, but the distances between the closest hydrogen atoms on the additional methyl group and on the C<sub>β</sub> atom are 2.29 Å in **36a** and 2.36 Å in **36d**. Because of the stronger repulsion in **36a** than in **36d**, the free energy increase from **35a** to **36a** is higher than that from **35d** to **36d**. These



structure	$\phi$	$\theta$	$\varphi$	$\psi$	structure	$\phi$	$\theta$	$\varphi$	$\psi$	structure	$\phi$	$\theta$	$\varphi$	$\psi$
<b>34a</b>	-169.3	62.2	68.5	-102.1	<b>36b</b>	-159.0	57.3	-88.4	124.7	<b>38c</b>	-79.9	-52.3	163.0	-93.6
<b>34b</b>	-163.7	61.6	-86.3	118.3	<b>36c</b>	-73.7	-62.7	167.2	-88.0	<b>38d</b>	-74.9	-50.1	71.4	-145.7
<b>34c</b>	-75.5	-61.4	167.1	-86.5	<b>36d</b>	-69.5	-56.9	71.9	-144.7	<b>38e</b>	-159.3	57.3	-57.3	167.6
<b>34d</b>	-70.3	-55.9	73.0	-147.2	<b>36e</b>	-116.4	59.5	-70.1	-71.4	<b>39a</b>	-161.9	62.3	69.7	-112.4
<b>34e</b>	-179.9	-61.3	-169.3	-147.7	<b>36f</b>	-155.8	67.4	-171.7	-178.7	<b>39b</b>	-165.9	61.2	69.5	-104.2
<b>35a</b>	-164.8	62.6	69.8	-106.3	<b>37a</b>	-166.6	59.9	67.1	-105.6	<b>39c</b>	-161.5	62.1	69.6	-110.9
<b>35b</b>	-159.8	58.0	-88.5	123.5	<b>37b</b>	-162.1	57.1	-88.2	122.5	<b>39d</b>	-159.5	56.6	-89.3	121.1
<b>35c</b>	-74.5	-62.1	166.7	-87.2	<b>37c</b>	-74.4	-61.9	167.1	-89.3	<b>39e</b>	-161.4	62.6	70.6	-112.9
<b>35d</b>	-70.6	-55.5	72.5	-146.3	<b>37d</b>	-66.0	-59.6	70.9	-142.6	<b>39f</b>	-73.3	-61.5	165.1	-87.6
<b>35e</b>	-117.7	60.4	-69.0	-71.9	<b>37e</b>	-158.5	65.8	-166.8	-171.2	<b>39g</b>	-64.4	-58.3	68.1	-134.2
<b>35f</b>	-156.8	66.6	-170.4	-175.8	<b>38a</b>	-166.0	59.5	69.2	-109.4	<b>39h</b>	-62.3	-58.1	75.0	-150.0
<b>36a</b>	-161.3	63.4	70.7	-108.1	<b>38b</b>	-166.9	62.7	-83.8	110.0					

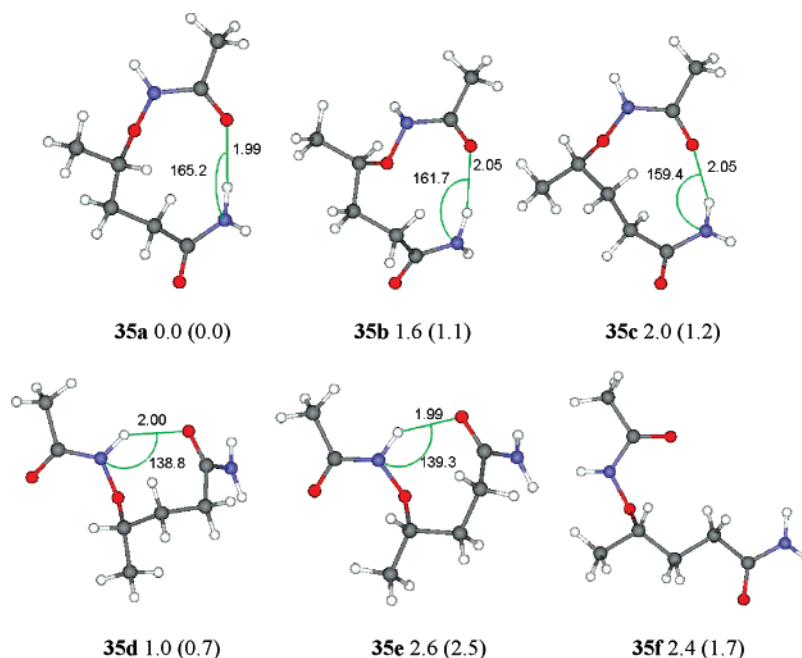


**Figure 8.** Calculated conformers of model compound **35**. The calculated relative free energies (kcal/mol) in the gas phase and in  $\text{CH}_2\text{Cl}_2$  (in parentheses) and the N–H···O hydrogen bond lengths and angles are provided.

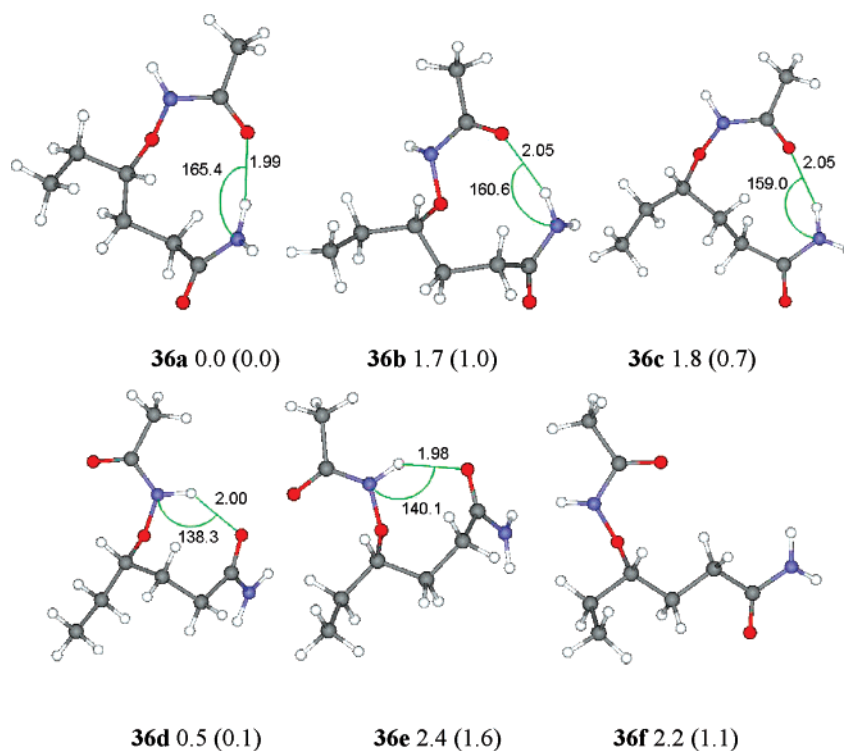


**Figure 9.** Calculated conformers of model compound **36**. The calculated relative free energies (kcal/mol) in the gas phase and in  $\text{CH}_2\text{Cl}_2$  (in parentheses) and the N–H···O hydrogen bond lengths and angles are provided.

results nicely explain our experimental observation that compound **27** having the (*S*)-configuration and an ethyl side chain adopts the left-handed 10-membered-ring hydrogen bond conformation (major) and the 8-membered-ring hydrogen bond

conformation (minor), and the 8-membered-ring hydrogen bond is more favorable in **27** than it is in **25** (stronger absorption at  $3241\text{ cm}^{-1}$  for **27** than that for **25**).

Figure 10 displays the five most stable conformations of model compound **37**, which has an (*R*)-configuration and a phenyl group at the  $\gamma^4$  position. Conformer **37a** is the most

- (31) Lyu, P. C.; Liff, M. I.; Marky, L. A.; Kallenbach, N. R. *Science* **1990**, *250*, 669–673.  
 (32) Oneil, K. T.; Degrado, W. F. *Science* **1990**, *250*, 646–651.  
 (33) Marqusee, S.; Robbins, V. H.; Baldwin, R. L. *Proc. Natl. Acad. Sci. U.S.A.* **1989**, *86*, 5286–5290.  
 (34) Rueping, M.; Schreiber, J. V.; Lelais, G.; Jaun, B.; Seebach, D. *Helv. Chim. Acta* **2002**, *85*, 2577–2593.

- (35) Raguse, T. L.; Lai, J. R.; Gellman, S. H. *J. Am. Chem. Soc.* **2003**, *125*, 5592–5593.  
 (36) Wang, X. F.; Espinosa, J. F.; Gellman, S. H. *J. Am. Chem. Soc.* **2000**, *122*, 4821–4822.

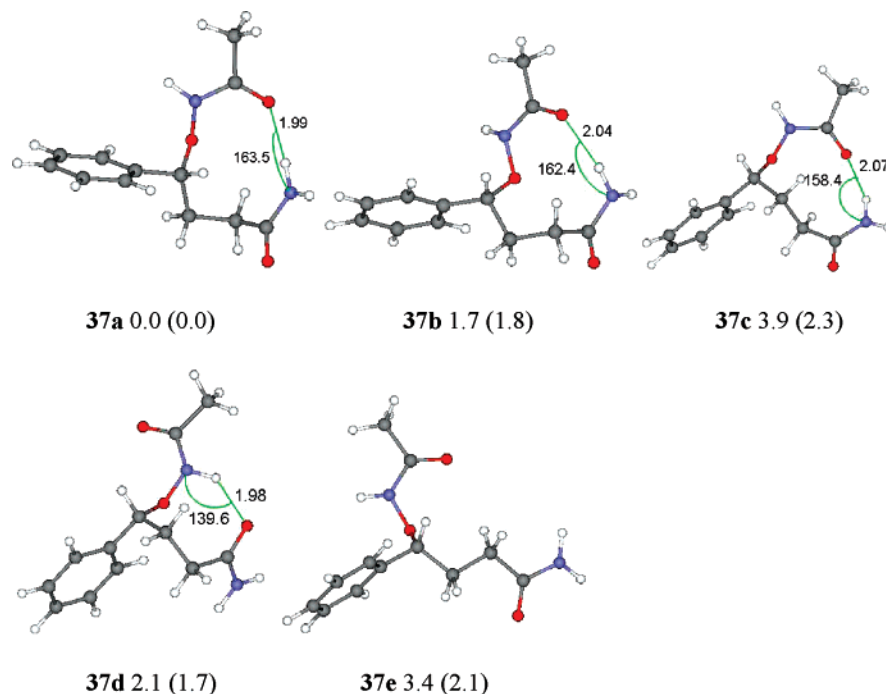


**Figure 10.** Calculated conformers of model compound **37**. The calculated relative free energies (kcal/mol) in the gas phase and in  $\text{CH}_2\text{Cl}_2$  (in parentheses) and the N–H···O hydrogen bond lengths and angles are provided.

stable with its 10-membered-ring hydrogen bond (hydrogen bond length: 1.99 Å; hydrogen bond angle: 163.5°). Conformers **37b** and **37c** are relatively less stable. Conformer **37b** suffers from severe distortion because of an unfavorable torsional angle  $\varphi$  (−88.2°). Conformer **37c** is much less stable than **37a** because of a combination of a bad torsional angle  $\phi$  (−74.4°) and a smaller angle between the phenyl ring and the C–O bond (25.6° in **37c**; 39.9° in **37a**), which leads to stronger steric repulsion in **37c** than in **37a**. Conformer **37d** with its eight-membered-ring hydrogen bond is also much less stable than **37a** because of the smaller angle between its phenyl ring and the C–O bond (19.5° in **37d**; 39.9° in **37a**). The energy difference between the dominant conformer **37a** and the other conformers is at least 1.7 kcal/mol, significantly larger than those for **35** and **36** because the phenyl ring is bulkier than either methyl or ethyl groups. These results reveal that the  $\gamma^4$ -aminoxy model compound **37** should strongly favor the 10-membered-ring hydrogen bond conformer **37a** and that the formation of the 10-membered-ring hydrogen bond in model compound **37** is more favorable than that in model compounds **35** and **36**.

Figure 11 displays the five most stable conformations of model compound **38**, in which the (*S*)- $\beta$  and (*S*)- $\gamma$  carbon atoms are part of a cis-disubstituted cyclohexyl ring. Conformer **38a** is the most stable with its 10-membered-ring hydrogen bond. Conformer **38b** is relatively less stable because of severe distortion of its torsional angle  $\varphi$  (−83.9°) caused by the

presence of the rigid cyclohexyl ring. Conformers **38c** and **38d** with their eight-membered-ring hydrogen bonds are less stable than **38a** because of their unfavorable torsional angles  $\phi$  and  $\theta$ . The energy difference between the dominant conformer **38a** and the other conformers is greater than 1.6 kcal/mol because the cyclohexyl side chain is bulky and rigid; in addition, the other conformers of **38** suffer from 4 more severe distortion than does **38a**. Therefore, the  $\gamma$ -aminoxy amide having a cis-disubstituted cyclohexyl side chain at its  $\beta$  and  $\gamma$  positions is predicted to strongly favor the 10-membered-ring intramolecular hydrogen bond conformer **38a**.

From our theoretical calculations of the model compounds **34**–**38**, we conclude that the  $\gamma^4$ -aminoxy peptides can form 10-membered-ring intramolecular hydrogen bonds ( $\gamma$  N–O turns) and that the extent of the hydrogen bond formation increases from the unsubstituted  $\gamma$ -aminoxy peptide to the  $\gamma^4$ -alkyl-substituted aminoxy peptides to the  $\gamma^{3,4}$ -cyclohexyl- and  $\gamma^4$ -Ph-substituted aminoxy peptides.

Figure 12 displays the four most stable conformations of the model compound **39**. Conformer **39a** is the most stable with its two contiguous left-handed  $\gamma$  N–O turn units, akin to the most stable conformer **35a**. Overall, **39a** corresponds to a helical structure, referred to as a  $\gamma$  N–O helix. Interestingly, the lengths of the hydrogen bond of **39a** are 1.90 and 1.95 Å, with hydrogen bond angles of 170.2 and 166.8°, respectively, which are better than those of **35a**. This finding indicates that the formation of the two 10-membered-ring hydrogen bonds in **39** is a cooperative process, in good agreement with the experimental observation that triamide **33** forms stronger intramolecular hydrogen bonds than does diamide **25**. Conformers **39b** and **39c** are less stable than **39a** because of the presence of less-stable  $\gamma$  N–O turn units (akin to that of **35b** in **39b** and **35c** in **39c**) in addition to one  $\gamma$  N–O turn unit akin to that in **35a**. Conformer **39d** has two contiguous eight-membered-ring hydrogen bond units (akin

(37) Yang, D.; Li, W.; Qu, J.; Luo, S. W.; Wu, Y. D. *J. Am. Chem. Soc.* **2003**, *125*, 13018–13019.

(38) Frisch, M. J.; et al. Gaussian 98, revision A.11.3, Gaussian, Inc.: Pittsburgh, PA, 2002.

(39) Becke, A. D. *J. Chem. Phys.* **1993**, *98*, 5648–5652.

(40) Lee, C.; Yang, W.; Parr, R. G. *Phys. Rev. B* **1988**, *37*, 785–789.

(41) Moller, C.; Plesset, M. S. *Phys. Rev.* **1934**, *46*, 618–622.

(42) Frisch, M. J.; Headgordon, M.; Pople, J. A. *Chem. Phys. Lett.* **1990**, *166*, 275–280.

(43) Frisch, M. J.; Headgordon, M.; Pople, J. A. *Chem. Phys. Lett.* **1990**, *166*, 281–289.

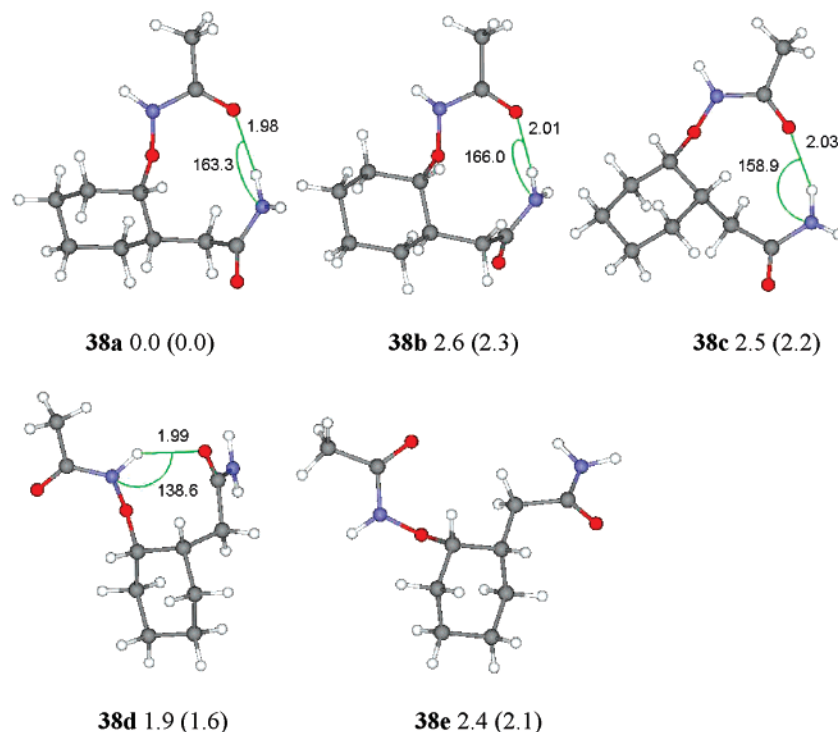


**Figure 11.** Calculated conformers of model compound **38**. The calculated relative free energies (kcal/mol) in the gas phase and in  $\text{CH}_2\text{Cl}_2$  (in parentheses) and the  $\text{N-H}\cdots\text{O}$  hydrogen bond lengths and angles are provided.

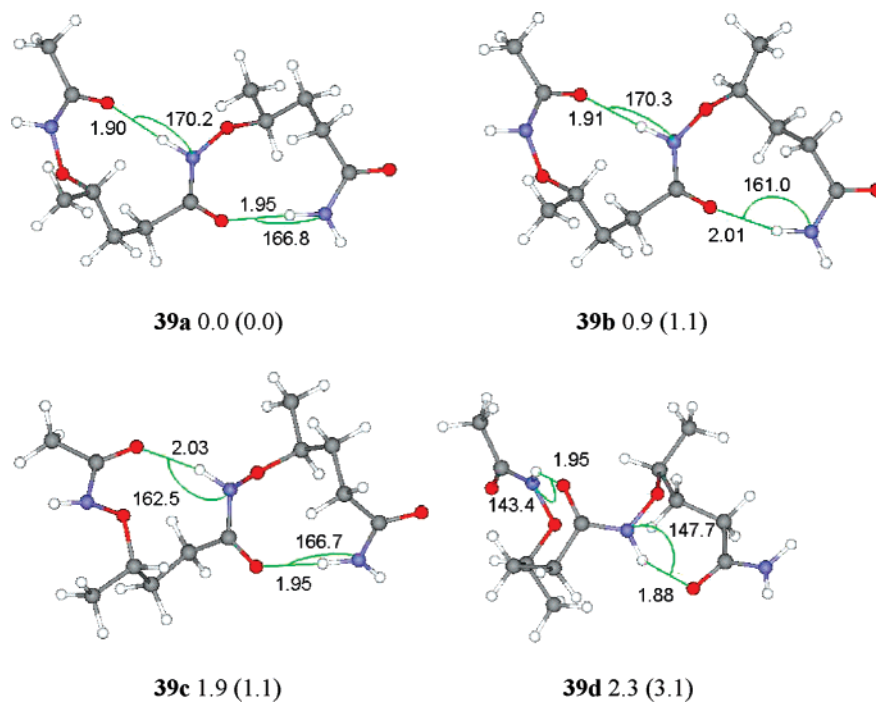


**Figure 12.** Calculated conformers of model compound **39**. The calculated relative free energies (kcal/mol) in the gas phase and in  $\text{CH}_2\text{Cl}_2$  (in parentheses) and the  $\text{N-H}\cdots\text{O}$  hydrogen bond lengths and angles are provided.

to that in **35d**) of the same handedness. This structure is calculated to be much less stable than structure **39a** because the torsional angles  $\phi$  ( $-64.4$  and  $-62.3^\circ$ , respectively) in **39d** are deviated greatly from that in **35d** ( $-70.6^\circ$ ). These results indicate that the (*S,S*)- $\gamma^4$ -aminoxy model peptide **39** should favor a helical structure formed from two left-handed  $\gamma$  N–O turn units akin to that in conformer **35a**.

## Conclusion

On the basis of experimental and theoretical findings for a series of  $\gamma$ -aminoxy peptides, namely those containing unsubstituted and  $\gamma^4$ -Ph-,  $\gamma^4$ -alkyl-, and  $\gamma^{3,4}$ -cyclohexyl-substituted aminoxy acid residues, we conclude that  $\gamma$ -aminoxy peptides can form 10-membered-ring intramolecular hydrogen bonds

between adjacent residues, that is,  $\gamma$  N–O turns. The extent of formation of the 10-membered-ring intramolecular hydrogen bonds increases from the unsubstituted  $\gamma$ -aminoxy peptide to the  $\gamma^4$ -alkyl-substituted aminoxy peptides to the  $\gamma^4$ -phenyl- and  $\gamma^{3,4}$ -cyclohexyl-substituted aminoxy peptides. The presence of two consecutive homochiral 10-membered-ring intramolecular hydrogen bonds results in the formation of a novel helical structure in which the formation of the consecutive  $\gamma$  N–O turns is a cooperative process. The experimental studies and theoretical calculations on  $\gamma$  N–O turns and  $\gamma$  N–O helices in  $\gamma$ -aminoxy peptides have provided many insights into the nature of folding of  $\gamma$ -aminoxy peptides. The understanding of the effect of the side chains on local conformational features of  $\gamma$ -aminoxy peptides should stimulate the design of new foldamers and their applications in drug development.

**Acknowledgment.** This study was supported by the University of Hong Kong and the Hong Kong Research Grants Council (grants HKU 7367/03M, HKU 2/06C, and HKUST 6083/02M). D.Y. acknowledges the Bristol-Myers Squibb Foundation for an unrestricted grant in Synthetic Organic Chemistry.

**Supporting Information Available:** Experimental details for the preparation and characterization of compounds **1–33**; HPLC traces for the determination of the values of ee of compounds **6**, **11**, and **19**; 2D-NOESY spectra of peptides **23**, **25**, and **29**; calculated relative energies of all  $\gamma$ -aminoxy peptides; calculated energies and corrections of all  $\gamma$ -aminoxy peptides; geometries (Cartesian coordinates) of all  $\gamma$ -aminoxy peptides optimized using B3LYP/6-31 (d, p); complete ref 38. This material is available free of charge via the Internet at <http://pubs.acs.org>.

JA0772750